PHILOSOPHICAL TRANSACTIONS OF THE ROYAL SOCIETY A

rsta.royalsocietypublishing.org

Research

Cite this article: Carlson RW, Borg LE, Gaffney AM, Boyet M. 2014 Rb-Sr, Sm-Nd and Lu-Hf isotope systematics of the lunar Mg-suite: the age of the lunar crust and its relation to the time of Moon formation. *Phil. Trans. R. Soc. A* **372**: 20130246. http://dx.doi.org/10.1098/rsta.2013.0246

One contribution of 19 to a Discussion Meeting Issue 'Origin of the Moon'.

Subject Areas:
geochemistry, solar system

Keywords:
lunar crust age, Moon formation, Mg-suite, magma ocean, giant impact

Author for correspondence:
Richard W. Carlson
e-mail: rcarlson@ciw.edu

Rb-Sr, Sm-Nd and Lu-Hf isotope systematics of the lunar Mg-suite: the age of the lunar crust and its relation to the time of Moon formation

Richard W. Carlson[1], Lars E. Borg[2], Amy M. Gaffney[2] and Maud Boyet[3]

[1]Department of Terrestrial Magnetism, Carnegie Institution of Washington, 5241 Broad Branch Road, NW, Washington DC 20015, USA
[2]Chemical Sciences Division, Lawrence Livermore National Laboratory, 7000 East Avenue L-231, Livermore, CA 94550, USA
[3]Laboratoire Magmas et Volcans, Universite Blaise Pascal, CNRS UMR 6524, 5 Rue Kessler, Clermont-Ferrand 63038, France

New Rb-Sr, ^{146,147}Sm-^{142,143}Nd and Lu-Hf isotopic analyses of Mg-suite lunar crustal rocks 67667, 76335, 77215 and 78238, including an internal isochron for norite 77215, were undertaken to better define the time and duration of lunar crust formation and the history of the source materials of the Mg-suite. Isochron ages determined in this study for 77215 are: Rb-Sr = 4450 ± 270 Ma, ^{147}Sm-^{143}Nd = 4283 ± 23 Ma and Lu-Hf = 4421 ± 68 Ma. The data define an initial ^{146}Sm/^{144}Sm ratio of 0.00193 ± 0.00092 corresponding to ages between 4348 and 4413 Ma depending on the half-life and initial abundance used for ^{146}Sm. The initial Nd and Hf isotopic compositions of all samples indicate a source region with slight enrichment in the incompatible elements in accord with previous suggestions that the Mg-suite crustal rocks contain a component of KREEP. The Sm/Nd—^{142}Nd/^{144}Nd correlation shown by both ferroan anorthosite and Mg-suite rocks is coincident with the trend defined by mare and KREEP basalts, the slope of which corresponds to ages between 4.35 and 4.45 Ga. These data, along with similar ages for various early Earth differentiation events, are in accord with the model of lunar formation via giant impact into Earth at *ca* 4.4 Ga.

Royal Society Publishing

1. Introduction

The time and duration of lunar highlands crust formation plays an unusually important role in models for lunar origin because of the suggestion that much of the highlands crust grew by plagioclase flotation from a crystallizing magma ocean [1]. In the magma ocean model for the Moon, an initially extensively molten Moon first crystallized mafic silicates that sank into the mantle to form the source regions of much later mare basalt magmatism [2,3]. After some 70–80% crystallization of the magma ocean, plagioclase began to crystallize from what was by then a dense iron-rich differentiated magma leading the plagioclase to float to form the ferroan anorthosite (FAN) clan of lunar highlands rocks [4]. The extraction of plagioclase from the magma ocean imprinted the later mafic cumulates in the lunar interior with a deficiency in Eu relative to neighbouring rare earth elements (REEs) that is reflected in the negative Eu anomalies of some mare basalts [5]. Further crystallization resulted in a residual liquid strongly enriched in incompatible elements that was given the name KREEP for its enrichment in potassium, REE and phosphorus, among many other incompatible elements [6]. The final component of the lunar highlands crust is a group of plagioclase-rich rocks that are distinguished from FANs by their higher Mg/Fe ratios, the presence of abundant mafic phases, and substantially higher incompatible element contents. This group of highlands rocks is known as the Mg-suite [7]. The parental magmas to the Mg-suite cumulate rocks usually are assumed to be partial melts of cumulates in the lunar interior [8], although an alternative is that the parental magmas originate from large impacts [9].

Where chronology enters the picture is that the magma ocean model predicts stratigraphic relationships in the rocks crystallized from the magma ocean. In this model, the mafic cumulate sources of the mare basalts form first, followed shortly by FANs, then by KREEP. The mare basalt source age and ferroan anorthosite age should be similar given the rapid crystallization of a magma ocean devoid of a thick, insulating crust [10]. Crystallization to the point of forming KREEP could take longer, perhaps up to 150 Ma [11], because of the high radioactive heat-producing capacity of KREEP and the fact that this last portion of magma ocean crystallization would take place with the surface boundary insulated by the thick highlands crust. If they indeed are later igneous intrusions into the crust, the Mg-suite rocks should yield ages no older than those of the FANs although a range to younger ages might be expected. Accurate chronology for lunar highlands rocks thus has the potential to test both whether the magma ocean model is correct and, if so, constrain the time of initial differentiation of the Moon.

Figure 1 illustrates that the age range of Mg-suite rocks is large and extends to relatively young (e.g. 4.18 Ga) ages. The oldest Mg-suite rocks overlap with the age range reported for FANs. How much of the age range of both the FANs and the Mg-suite reflects the true range of crystallization ages of crustal rocks as opposed to later metamorphic disturbance has been the subject of much work [14,21,23,28,29]. Obtaining convincingly accurate and adequately precise ages for lunar crustal rocks has proved difficult. Neither the Mg-suite nor FANs contain high closure temperature U-rich minerals, such as zircon that has proved itself as a precise and accurate chronometer of igneous rock crystallization. FANs have extremely low incompatible element contents, and because all the long-lived radioactive chronometers, except Re-Os, involve incompatible elements, analyses of FANs are unusually susceptible to both laboratory blank and natural contamination. FANs also are composed primarily of plagioclase, to the point that the presence of even minor mafic phases is interpreted as a sign of a polymict nature [30]. Mg-suite samples have much higher incompatible element abundances and mafic phases that clearly crystallized from the same parental magma as the plagioclase. Many Mg-suite samples show evidence of shock metamorphism including formation of maskelynite and the presence of impact melt glass. Finally, exposure of the lunar surface to cosmic ray irradiation produces secondary neutrons that can substantially influence the isotopic composition of samples that have long exposure histories, with important consequences for ^{146}Sm-^{142}Nd and Lu-Hf results [31–35].

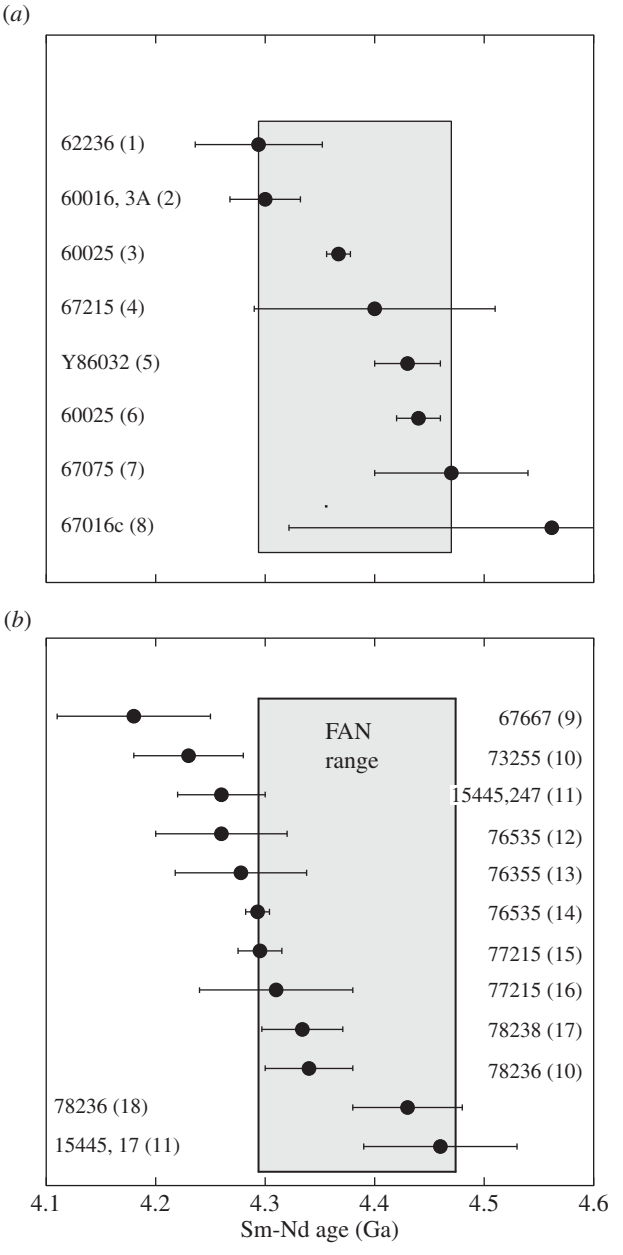

Figure 1. Sm-Nd isochron ages for rocks from the (*a*) FAN and (*b*) Mg-suite groups of highlands rocks. Data from: 1—Borg *et al.* [12]; 2—Marks *et al.* [13]; 3—Borg *et al.* [14]; 4—Norman *et al.* [15]; 5—Nyquist *et al.* [16]; 6—Carlson & Lugmair [17]; 7—Nyquist *et al.* [18]; 8—Alibert *et al.* [19]; 9—Carlson & Lugmair [20]; 10—Carlson & Lugmair [21]; 11—Shih *et al.* [22]; 12—Lugmair *et al.* [23]; 13—Edmunson *et al.* [24]; 14—Borg *et al.* [25]; 15—this study; 16—Nakamura *et al.* [26]; 17—Edmunson *et al.* [27] and 18—Nyquist *et al.* [28].

Given these issues and the importance of lunar crustal chronology to the understanding of Moon formation and early differentiation, we have been revisiting the lunar highlands sample collection in order to apply modern analytical approaches that involve several different isotope systems and the improved precision of modern mass spectrometric techniques in an attempt better illuminate the correct interpretation of both the ages and initial isotopic compositions

of lunar highlands rocks. This paper reports results for Rb-Sr, ^{146,147}Sm-^{142,143}Nd and Lu-Hf measurements of whole rock samples of feldspathic lherzolite 67667, cataclastic magnesian anorthosite 76335 and norite 78238 along with minerals separated from the Mg-suite norite 77215 and compares the results with recent data for other highlands rocks to derive constraints on the early history of the Moon.

2. Sample descriptions and previous chronological results

Troctolitic anorthosite 76335 consists of 88% plagioclase and 12% olivine with a number of trace phases including minor orthopyroxene, chromite and phosphate [36]. 76335 provided a Sm-Nd age of 4278 ± 60 Ma with an initial ε^{143}Nd of 0.06 ± 0.39, but the rock has been significantly shocked as indicated by disturbed Rb-Sr systematics [24]. Cumulate norite 78238 is one of several (78235–78238) that were sampled from a glass covered noritic boulder at Apollo 17, station 8. The rocks are about 50 : 50 plagioclase and orthopyroxene with accessory minerals including clinopyroxene, phosphates and veins of shock-melted glass [37]. This group of rocks have been the subject of many chronological investigations including Ar-Ar (4.11 ± 0.02 Ga, [38]); Rb-Sr (4.38 ± 0.02, [28]; 4.37 ± 0.05, [27]); Sm-Nd (4.43 ± 0.05 Ga, [28]; 4.34 ± 0.04 Ga, [21]; 4.33 ± 0.04 Ga, [27]) and U-Pb (4.43 ± 0.06 Ga, [39]), all of which show disturbance due to the shock this rock has experienced. Apollo 16 feldspathic lherzolite 67667 consists of 50% olivine, 21% orthopyroxene, 5% clinopyroxene, 23% plagioclase and 1% ilmenite [40]. As with most highlands samples, 67667 displays ample evidence of shock. 67667 has been dated by Sm-Nd at 4.18 ± 0.07 Ga with an initial ε^{143}Nd of 0.8 ± 1.6 [20].

Apollo 17 sample 77215 consists of a number of brecciated pigeonite-anorthite cumulate clasts cut and surrounded by melt rock. Chao *et al.* [41] concluded that 77215 crystallized and cooled slowly at a depth of approximately 10 km and was then excavated by an impact and mixed with impact melts of similar noritic composition. They suggest further that 77215 may have been derived from the same parental magma as 78238 and related norites. Ar-Ar study of subsample 77215, 45a provided ages of 3.96 to 4.05 Ga, interpreted as the time of impact excavation [42]. Nakamura *et al.* [26] reported Rb-Sr and Sm-Nd results for 77215. Correcting their data to a value of ^{87}Sr/^{86}Sr = 0.71025 for the NIST-987 standard and refitting the data using Isoplot [43] and a ^{87}Rb decay constant of 1.402×10^{-11} yr^{-1} [44], their Rb-Sr results for all splits define a scattered array (MSWD = 203) with slope corresponding to an age of 4313 ± 320 Ma with initial ^{87}Sr/^{86}Sr = 0.6997 ± 0.0012 (errors at the 95% confidence level). The two high-density separates analysed are the primary cause of scatter on the isochron. Excluding these two points from the line fitting, the remaining eight data points define a reasonably precise (MSWD = 2.6) isochron of age 4371 ± 52 Ma with initial ^{87}Sr/^{86}Sr = 0.69910 ± 0.00013.

Accounting for interlaboratory bias in the Sm-Nd data of Nakamura *et al.* [26] is difficult for a number of reasons. They report data for a variety of standards, but none of the standards measured in the USGS laboratory at that time were measured by other groups, making it impossible to directly compare measured ^{143}Nd/^{144}Nd data. Their Nd data are fractionation corrected to ^{142}Nd/^{146}Nd, which is sensitive to interference from ^{142}Ce and also propagates the variable ^{142}Nd abundance caused by decay of ^{146}Sm into the ^{143}Nd/^{144}Nd ratio. Nakamura *et al.* [26] report significant ^{142}Ce interferences in the range of 10^{-4}–10^{-5}. The effect of variable ^{142}Nd is small because of the limited ^{142}Nd variation in a lunar rock of this age. With their fractionation scheme, the ^{146}Nd/^{144}Nd they measure in standards is 0.72198, which is higher than the 0.7219 value now used by most workers for fractionation correction of Nd isotope ratios. Re-correcting their data for mass fractionation to ^{146}Nd/^{144}Nd = 0.7219 will raise their reported ^{143}Nd/^{144}Nd values by a factor of 1.000055. Nakamura *et al.* [26] report data for a whole rock aliquot of the Juvinas eucrite, which can serve as another comparison with modern Sm-Nd data assuming that the Juvinas point lies on a 4.56 Ga isochron that passes through the average chondrite data of Bouvier *et al.* [45]. The Nakamura *et al.*'s [26] data for Juvinas, however, plot above the 4.56 Ga isochron because either ^{143}Nd/^{144}Nd is too high by a factor of 1.000155, or ^{147}Sm/^{144}Nd is

too low by a factor of 1.0136. Ignoring the correction suggested by the Juvinas comparison, their Sm-Nd data for mineral separates and whole rock aliquots from 77215 provide a Sm-Nd isochron age of 4373 ± 69 Ma (MSWD = 1.0) with initial $\varepsilon^{143}Nd = -2.8 \pm 2.2$. Using the Juvinas comparison and increasing their reported $^{147}Sm/^{144}Nd$ ratios by a factor of 1.0136 causes the data to define an isochron of 4316 ± 68 Ma with initial $\varepsilon^{143}Nd = -4.3 \pm 2.2$. Although problematic, the Nakamura *et al.*'s [26] data imply that the Sm-Nd crystallization age of 77215 is between 4.32 and 4.37 Ga.

Nunes *et al.* [46] report U-Pb results for whole rock and mineral separates from 77215. Recalculating their results using Isoplot provides a highly scattered Pb-Pb array of age 4417 ± 130 Ma using all data points. At the radiogenic end of the array, data for pyroxene have substantially lower $^{207}Pb/^{206}Pb$ at higher $^{206}Pb/^{204}Pb$ than do whole rock measurements. A line fit to the whole rock and plagioclase data alone provides an age of 4377 ± 210 Ma (MSWD = 22), while a line fit to the plagioclase and pyroxene data alone provides an age of 4007 ± 360 Ma (MSWD = 1055). Both the scatter and young age of the pyroxene-plagioclase tie line suggest substantial disturbance of the U-Pb system in the mafic phases of 77215, something that is also observed in the Rb-Sr data of Nakamura *et al.* [26].

3. Procedures

Whole rock chips were crushed to powder in an agate mortar. A 143 mg aliquot of 77215 was crushed in an agate mortar and sieved to obtain 71.6 mg of a size fraction between 106 and 250 μm. The less than 106 μm fraction was used both for the total-spiked whole rock measurement with a separate aliquot (26.2 mg) dissolved and processed without spike. The sieved fraction was passed through a Frantz isodynamic separator in order to separate plagioclase from mafic phases. The final non-magnetic fraction consisted primarily of plagioclase with a small percentage of black grains that were removed by hand picking. The pyroxene fraction contained a fair amount of plagioclase and so was crushed further, sieved and passed again through the Frantz magnetic separator followed by a final handpicking to remove impurities.

Samples were weighed into 15 ml Savillex PFA Teflon beakers to which appropriate quantities of isotopically enriched ^{87}Rb, ^{84}Sr and mixed ^{150}Nd-^{149}Sm and ^{176}Lu-^{178}Hf spikes were added. For this work, a highly enriched ^{150}Nd (99.988 atom %) spike was used that allowed determination of the $^{142}Nd/^{144}Nd$ ratio for total-spiked samples with only minor correction needed for spike contribution to the isotopic composition. This newly prepared mixed Sm-Nd spike was calibrated against the same standard solutions prepared from AMES Sm and Nd metal used in the work of Boyet & Carlson [47]. The most recent calibration of the Lu-Hf spike, done in September 2013, showed Lu and Hf concentration reproducibility in four independent calibrations of 0.12% and 0.04%, respectively.

A blank, treated identically to the samples, but without sample added, was run in parallel with the samples. Sample digestion followed procedures described in Carlson *et al.* [48] and Boyet & Carlson [47]. The total procedural blank measured during this analysis period is Rb = 318 pg, Sr = 91 pg, Nd = 10 pg, Sm = 1.9 pg, Lu = 1.6 pg and Hf = 50 pg. These blanks are less than 0.12% of the analysed sample amounts for all Sr, Sm, Nd, Lu and Hf analyses. Rb blanks are less than 0.3–2.7% (77215 pyroxene) of the analysed amounts. Blank corrections have been made for all analyses.

A second whole rock Lu-Hf analysis of 77215 was performed at LLNL on a separate sample aliquot. After complete dissolution using Parr digestion vessels, the sample was split and one aliquot was spiked with a mixed ^{180}Hf-^{176}Lu tracer. Hafnium was purified following the procedures of Connelly *et al.* [49]. The REE cut from the cation exchange column was passed through an α-hydroxyisobutyric acid column (0.1 M, pH = 4.10) to purify Lu. Purified Hf and Lu were analysed on the Nu Plasma HR MC-ICP-MS at LLNL.

Sr, Nd and Sm isotopic compositions were measured on the DTM Thermo-Fisher Triton thermal ionization mass spectrometer using procedures similar to those described in Carlson

et al. [50] and Qin *et al.* [51]. Each Sr ratio involved 8-s integrations with amplifier rotation used during runs of 262 (77215 pyroxene) to 400 (all other samples) ratios. Signal strengths of ^{88}Sr ranged from 2.5×10^{-11} amps for 77215 pyroxene to 10–17 $\times 10^{-11}$ amps for all other samples.

Nd was analysed as Nd^+ from double Re filaments using a two-step dynamic routine described in Carlson *et al.* [50]. The 77215 analyses involved ^{144}Nd signal sizes of approximately 1.6×10^{-11} amps for a total of 240 ratios for pyroxene, 270 ratios for plagioclase and 360 ratios for the whole rock. All other whole rock analyses used ^{144}Nd signal sizes of approximately 2×10^{-11} amps for 270 (67667), 960 (76335) or 1620 (78238) ratios. Average ratios for four runs of the JNdi standard run with the whole rocks (except 77215) are $^{142}Nd/^{144}Nd = 1.141839 \pm 0.000011$ and $^{143}Nd/^{144}Nd = 0.512109 \pm 0.000006$ (errors are 2σ). The averages for three filaments of the JNdi standard run 1 year later in the same barrel as the 77215 samples are $^{142}Nd/^{144}Nd = 1.141840 \pm 0.000006$ and $^{143}Nd/^{144}Nd = 0.512118 \pm 0.000005$. The $^{143}Nd/^{144}Nd$ ratios measured for the samples are adjusted to a value of 0.512115 for the JNdi standard, which is equivalent to $^{143}Nd/^{144}Nd = 0.511853$ for the La Jolla Nd standard as determined on consecutive runs of the JNdi and La Jolla standards. $^{147}Sm/^{146}Nd$ was 2×10^{-6} or lower for most runs with the exception of 78238 (2×10^{-5}) and 77215 pyroxene (1.1×10^{-5}). $^{140}Ce/^{146}Nd$ was less than 5×10^{-5} for most whole rocks and the 77215 pyroxene, but was 1.3×10^{-4} for plagioclase and 3.5×10^{-4} for 76335 whole rock. Corrections for ^{142}Ce interference on ^{142}Nd were applied for all samples.

Signal sizes of ^{152}Sm of 0.8–1.5 $\times 10^{-11}$ amps were obtained for all samples with the data reflecting the average of 120 ratios taken with 8 s integrations using amplifier rotation. Mass fractionation was corrected to $^{147}Sm/^{152}Sm = 0.56081$ and to $^{147}Sm/^{154}Sm = 0.65916$, the latter to check on the possibility of production of ^{152}Sm via neutron capture on ^{151}Eu. Using this latter fractionation correction, after spike correction, no sample displayed $^{152}Sm/^{154}Sm$ ratios more than three parts in 10 000 higher than the standard. Given this minimal, if any, effect on the ^{152}Sm relative abundance due to neutron exposure, Sm concentrations were calculated using the $^{147}Sm/^{152}Sm$ fractionation correction. The Sm isotopic composition measured for an unspiked aliquot of 77215 whole rock (table 1) shows no resolvable deficit in ^{149}Sm. Unspiked aliquots of Sm from 78238 and 76535 were measured in separate studies [25,34] and showed $\varepsilon^{149}Sm$ of −27.4 and −13.5, respectively, relative to terrestrial Sm. After correction for the spike contribution to ^{150}Sm (table 1), and using the ^{150}Sm–^{149}Sm relationship for lunar samples with significant neutron capture histories from Boyet & Carlson [52], the estimated $\varepsilon^{149}Sm$ calculated from the spiked runs were −27.0, −12.3 and −3.0 for 78238, 76355 and 67667, respectively. For calculating the Sm concentration and the corrections for neutron capture on ^{142}Nd, the measured unspiked ^{149}Sm values were used for 77215 and 78238, while for 76335 and 67667, the estimates of the ^{149}Sm deficit obtained from the spike-corrected ^{150}Sm values measured in this study were used. The neutron exposure of these samples required negligible corrections for 77215 and 67667, but the significant neutron exposures seen by 76335 and 78238 required corrections to $^{142}Nd/^{144}Nd$ of 11 and 22 ppm, respectively, using the approach of Rankenburg *et al.* [32].

Rb, Lu and Hf were measured on the DTM Nu-Plasma-HR, multicollector ICP-MS. Instrumental mass fractionation for Rb and Lu was corrected using standards interspersed with the sample analyses. Signal sizes for ^{85}Rb were 0.6–2.8 $\times 10^{-11}$ amps for all samples except 77215 pyroxene (7.9×10^{-13} amps). Lu signal sizes were between $^{175}Lu = 0.4$ and 2×10^{-11} amps for all whole rocks, but only 6.5×10^{-13} amps for 77215 pyroxene and 1.5×10^{-13} amps for 77215 plagioclase.

Solutions containing Hf were aspirated into the ICP-MS using an MCN-6000 desolvating nebulizer and 50 µl min^{-1} Teflon nebulizer. Signal sizes of ^{178}Hf were between 1.5 and 6×10^{-11} amps. Measured ratios of the monitored interferences to the ^{177}Hf signal did not exceed 0.00006 for any sample. Ratios are calculated statically using 10 s integrations. Most samples were run for 80 ratios with the exception of 77215 whole rock and plagioclase (55 ratios) and 77215 pyroxene (49 ratios). Seven runs of the JMC-475 Hf standard run with all whole rocks but 77215 produced an average $^{176}Hf/^{177}Hf = 0.282145 \pm 0.000003$. Five runs of the same standard run during the 77215 analytical session provided an average $^{176}Hf/^{177}Hf = 0.282138 \pm 0.000010$.

Table 1. Sm and Hf isotopic composition. Sm fractionation corrected to $^{147}Sm/^{152}Sm = 0.56081$, Hf to $^{179}Hf/^{177}Hf = 0.7325$ with $^{176}Hf/^{177}Hf$ reported relative to 0.282160 for the JMC-475 Hf standard. Spike-corrected ratios reflect the values after stripping spike contribution, but the primary spiked isotope ratios ($^{149}Sm/^{152}Sm$ and $^{178}Hf/^{177}Hf$) are reported as measured. ε is the deviation in parts in 10 000 from the value of the ratio in the standard.

	$^{144}Sm/^{152}Sm$	$^{148}Sm/^{152}Sm$	$^{149}Sm/^{152}Sm$	$^{150}Sm/^{152}Sm$	$^{154}Sm/^{152}Sm$	*n*	
standard (DTM)	0.114946	0.420419	0.516840	0.275981	0.850812	2	
2σ	0.000015	0.000010	0.000011	0.000008	0.000012		
standard (LLNL)	0.114997	0.420438	0.516853	0.275993	0.850792	54	
2σ	0.000007	0.000013	0.000001	0.000005	0.000026		
						$\varepsilon^{149}Sm$	$\varepsilon^{150}Sm$
unspiked 77215 (DTM)	0.114968	0.420444	0.516841	0.276036	0.850795	0.02	2.00
2σ	0.000003	0.000004	0.000005	0.000003	0.000008	0.09	0.11
78238 (LLNL)	0.114986	0.420446	0.515437	0.277383	0.850658	−27.4	50.8
2σ	0.000002	0.000003	0.000003	0.000002	0.000005	0.06	0.07
spike corrected							
77215WR	0.114973	0.420440	0.911588	0.276084	0.850760	7638	3.73
77215Px	0.114962	0.420421	0.780324	0.275978	0.850758	5098	−0.11
77215Pl	0.114985	0.420434	0.720466	0.276051	0.850735	3940	2.53
67667	0.114971	0.420432	0.827814	0.276177	0.850772	6017	7.10
76355	0.115005	0.420428	0.810244	0.276660	0.850594	5677	24.61
78238	0.114979	0.420449	0.777587	0.277428	0.850697	5045	52.42
	$^{174}Hf/^{177}Hf$	$^{176}Hf/^{177}Hf$	$^{178}Hf/^{177}Hf$	$^{180}Hf/^{177}Hf$	$\varepsilon^{180}Hf$		
standard	0.008653	0.282138	1.467481	1.886825			
2σ	0.000006	0.000010	0.000051	0.000079	0.42		
spike corrected							
77215WR	0.008658	0.282778	1.504768	1.886893	0.36		
77215Px	0.008647	0.282601	1.569252	1.886919	0.50		
77215Pl	0.008633	0.281421	1.477830	1.886838	0.07		
76355	0.008663	0.281029	1.499380	1.886738	−0.46		
78238	0.008661	0.282554	1.536428	1.886611	−1.13		
67667	0.008655	0.282187	1.515238	1.886896	0.38		

The stable Hf isotope compositions, after spike correction, for each sample are reported in table 1. Given the limited neutron exposure of 77215 and 67667, concentration and spike correction calculations for these two samples were done assuming stable Hf isotopic compositions equal to those of the terrestrial standard. For 78238 and 76355, concentration calculations were done iteratively first using terrestrial standard Hf, then a Hf isotopic composition adjusted for the $^{180}Hf/^{177}Hf$ calculated from the spike corrected value found in the first iterative step. In this second step, the deviation of the sample's $\varepsilon^{178}Hf$ from the standard was assumed to equal 0.607 times that of the $\varepsilon^{180}Hf$ based on fitting the lunar basalt data from Sprung *et al.* [35]. Using the same dataset, the neutron correction to $\varepsilon^{176}Hf = 1.64^{*}\varepsilon^{180}Hf$ and is therefore −0.82 for 76335 and −2.0 for 78238.

Table 2. Isotopic results for Mg-suite samples. Sr isotopic composition fractionation corrected to $^{86}Sr/^{88}Sr = 0.1194$. The average value for $^{87}Sr/^{86}Sr$ obtained for NIST-987 Sr = 0.7102561 ± 0.0000013 ($n = 5$), but the data in the table are reported relative to a value of 0.71025. Nd is fractionation corrected to $^{146}Nd/^{144}Nd = 0.7219$, with $^{143}Nd/^{144}Nd$ reported relative to a value of 0.512115 for the JNdi Nd standard. Hf is fractionation corrected to $^{179}Hf/^{177}Hf = 0.7325$ and reported relative to a value of $^{176}Hf/^{177}Hf = 0.282160$ in the JMC-475 Hf standard. All fractionation correction is done assuming exponential mass dependency. $^{142}Nd/^{144}Nd$ and $^{176}Hf/^{177}Hf$ are corrected for neutron capture as explained in the text. The LLNL Hf isotopic data were measured on an unspiked aliquot.

	77215 WR	77215-WR (LLNL)	77215 Plag	77215 Px	78238 WR	76355 WR	67667 WR
weight (g)	0.0685	0.1200	0.0159	0.0128	0.0911	0.1372	0.0742
[Rb] ppm	2.67		6.59	1.09	1.40	0.998	0.587
[Sr] ppm	92.6		216	7.80	83.8	157	117
$^{87}Rb/^{86}Rb$	0.0834		0.0884	0.4041	0.0483	0.0183	0.0145
$^{87}Sr/^{86}Sr$	0.704124		0.704723	0.724811	0.702287	0.700235	0.700043
2σ	0.000004		0.000003	0.000010	0.000004	0.000004	0.000004
[Sm] ppm	3.520		8.350	2.224	2.425	1.104	2.812
[Nd] ppm	12.13		47.78	6.082	8.386	3.689	8.805
$^{147}Sm/^{144}Nd$	0.1754		0.1566	0.2210	0.1748	0.1810	0.1930
$^{143}Nd/^{144}Nd$	0.512016		0.511491	0.513320	0.511988	0.512171	0.512538
2σ	0.000004		0.000004	0.000005	0.000001	0.000002	0.000004
$^{142}Nd/^{144}Nd$	1.141812		1.141806	1.141831	1.141816	1.141817	1.141829
2σ	0.000008		0.000007	0.000010	0.000003	0.000004	0.000008
[Lu] ppm	0.642	0.671	0.444	0.897	0.370	0.115	0.395
[Hf] ppm	2.700	3.483	3.501	3.988	1.687	1.258	2.112
$^{176}Lu/^{177}Hf$	0.03375	0.02734	0.01801	0.03193	0.0311	0.0130	0.0266
$^{176}Hf/^{177}Hf$	0.282778	0.282240	0.281421	0.282601	0.282554	0.281029	0.282187
2σ	0.000006	0.000010	0.000006	0.000009	0.000003	0.000005	0.000004

Results are reported in table 2. All line fitting in this paper is done using Isoplot [43]. Uncertainties assigned to Rb/Sr and Sm/Nd ratios are 0.1% and 0.5%, respectively. Given the small Lu signal sizes obtained for the 77215 mineral separates, the Lu/Hf ratios for the separates are assigned an error of 1% compared with the typical 0.5% for the whole rocks. Age uncertainties are reported at the 95% confidence level. Decay constants used for calculating ages are $^{87}Rb = 1.402 \times 10^{-11}\,yr^{-1}$ [44], $^{147}Sm = 6.54 \times 10^{-12}\,yr^{-1}$ [53] and $^{176}Lu = 1.867 \times 10^{-11}\,yr^{-1}$ [54,55]. ^{146}Sm-^{142}Nd ages will be compared using decay constants of $6.73 \times 10^{-9}\,yr^{-1}$ [56] with Solar System initial $^{146}Sm/^{144}Sm = 0.0084$ [57] and the more recently measured value of $1.02 \times 10^{-8}\,yr^{-1}$ [58], which requires the Solar System initial $^{146}Sm/^{144}Sm$ to be adjusted to 0.0094. Chondrite reference parameters used in this paper are $^{147}Sm/^{144}Nd = 0.196$, $^{143}Nd/^{144}Nd = 0.51263$, $^{176}Lu/^{177}Hf = 0.0336$ and $^{176}Hf/^{177}Hf = 0.282785$ from Bouvier *et al.* [45]. Uncertainties on initial Nd and Hf isotopic compositions are calculated using the approach of Fletcher & Rosman [59].

4. Results

The Sm-Nd data for 77215 define a ^{147}Sm-^{143}Nd isochron of 4283 ± 23 Ma age (MSWD = 3.0) and initial $^{143}Nd/^{144}Nd = 0.507039 \pm 0.000027$ for an initial $\varepsilon^{143}Nd = -0.35 \pm 0.09$ (figure 2). The data also define a good linear correlation in Sm/Nd versus $^{142}Nd/^{144}Nd$ although the total range

in $^{142}Nd/^{144}Nd$ is only 22 ppm. The slope of the line corresponds to an initial $^{146}Sm/^{144}Sm = 0.00193 \pm 0.00092$ and an initial $^{142}Nd/^{144}Nd = 1.141744 \pm 0.00006$ corresponding to $\varepsilon^{142}Nd = -0.16 \pm 0.05$ relative to terrestrial Nd at that time. Using the 103 Ma half-life and Solar System initial $^{146}Sm/^{144}Sm = 0.0084$, the slope corresponds to an age of 4348^{+57}_{-96} Ma. The age is calculated to be 4413^{+38}_{-63} Ma when using the half-life from Kinoshita *et al.* [58]. The data reported here are clearly offset to higher $^{143}Nd/^{144}Nd$, or lower Sm/Nd, compared with the data reported by Nakamura *et al.* [26]. All of the Mg-suite whole rocks, except for 67667, lie within uncertainty of the ^{146}Sm-^{142}Nd line defined by 77215 (figure 2*b*), but are not used in the age calculation for 77215.

The four Lu-Hf data for 77215 define a linear array (MSWD = 2.6) with a slope that corresponds to an age of 4421 ± 68 Ma with initial $^{176}Hf/^{177}Hf = 0.27988 \pm 0.00004$ or initial $\varepsilon Hf = -0.5 \pm 1.4$ (figure 3). The whole rock fraction measured here has a Lu/Hf ratio that does not lie between those of the pyroxene and plagioclase. The three other whole rock Mg-suite data also have been plotted on the 77215 isochron diagram in figure 3, but were not used in the calculation of the 77215 isochron. The whole rock data lie between 0.2 and 1.0 ε above the 77215 isochron, suggesting that these Mg-suite samples share a similar petrogenetic history. Leaving out the much younger 67667, the remaining four whole rock data, for rocks with overlapping internal isochron ages, define a line that corresponds to an age of 4347 ± 29 Ma (MSWD = 0.3) and initial $^{176}Hf/^{177}Hf = 0.279930 \pm 0.000013$ ($\varepsilon Hf = -0.5 \pm 0.5$).

The 77215 mineral data define a three point Rb-Sr best fit line with slope corresponding to an age of 4450 ± 270 Ma (MSWD = 2) with initial $^{87}Sr/^{86}Sr = 0.69888 \pm 0.00042$ (figure 4). At the low Rb/Sr end of the isochron, the whole rock and plagioclase separates do not plot on the isochron within uncertainty. They define two-point tie lines of 4400 Ma (plagioclase) and 4459 Ma (whole rock) with the pyroxene data. In the three data reported here, as with Lu-Hf, the whole rock has a Rb/Sr ratio that does not lie between the Rb/Sr ratios of the mineral separates implying that there is a phase in the whole rock with sufficiently low Rb/Sr and high Sr content compared with plagioclase to account for the offset of the whole rock point from the plagioclase separate. Our plagioclase separate also has substantially higher Rb/Sr ratio than did the plagioclase analysed by Nakamura *et al.* [26]. Including the data from Nakamura *et al.* [26], after adjusting to a value of NIST-987 = 0.710250 and assigning an uncertainty of ±1% to their reported Rb/Sr ratios, the combined dataset defines an isochron of 4374 ± 45 Ma (MSWD = 2.1) and initial $^{87}Sr/^{86}Sr = 0.69908 \pm 0.00011$, leaving off their two high-density mineral separates, which lie well above the line defined by the remaining samples. The other three Mg-suite whole rocks analysed here fall close to the 77215 mineral isochron but are not included in the age determination for 77215.

5. Discussion

(a) 77215 mineral systematics

The small size (143 mg) of the starting sample used here and that (70 mg) used in the study of Nakamura *et al.* [26] make it unlikely that the 'whole rock' aliquots actually represent the whole rock composition of the 77215 norite. Nevertheless, the Rb and Sr concentrations for the whole rock splits from the two studies are within 14% and 7%, respectively. While the Sm and Nd concentrations differ by 22–24% between the two studies, the whole rock Sm/Nd ratios differ by only 1.7%. The greatest difference between our and the Nakamura *et al.*'s [26] data is for the Sm and Nd concentration of plagioclase. Our plagioclase separate has approximately twice as much Sm and Nd as did the plagioclase separate analysed by Nakamura *et al.* [26], but with nearly identical Sm/Nd ratios. Chao *et al.* [41] list an approximate mode for 77215 of 51.8% plagioclase, 44.6% orthopyroxene and a number of phases present at approximately 1% or less. With this mode, the Nd concentrations measured here for plagioclase and pyroxene would lead to a whole rock with approximately 19 ppm Nd, some 60% higher than the measured value. We interpret this

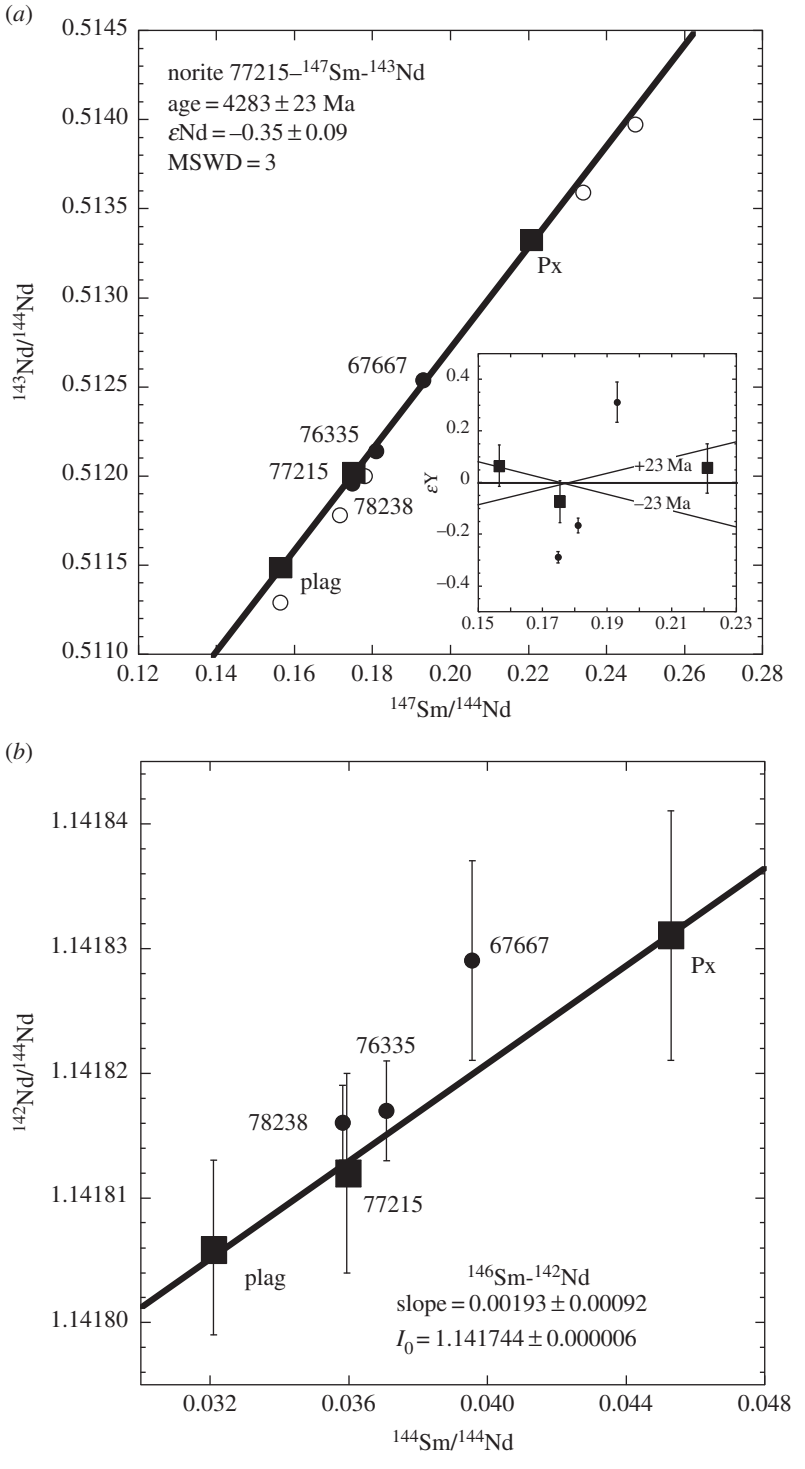

Figure 2. Sm-Nd isochron diagrams for 77215. Data measured here for 77215 are shown by filled squares along with the data for other Mg-suite whole rocks (filled circles). The open circles are the data from Nakamura *et al.* [26] that are as reported in that study after refractionation correction to $^{146}Nd/^{144}Nd = 0.7219$. The inset to part (*a*) shows the deviation of the individual points, in parts in 10 000 from the 77215 internal isochron.

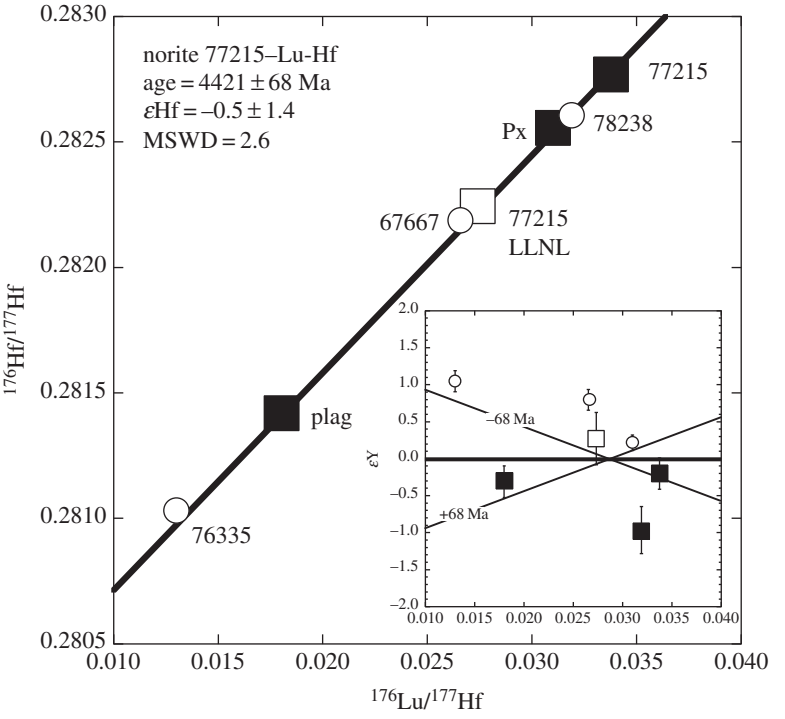

Figure 3. Lu-Hf isochron diagram for 77215 minerals and whole rock (squares) and other Mg-suite samples (circles). The open square denotes the 77215 whole rock sample measured at LLNL. The inset shows deviations of the data, in parts in 10 000 from the 77215 internal isochron. Only the data for 77215 are used to determine the lines shown in the figure.

combination of observations to suggest that our plagioclase separate contained a REE-rich phase in addition to plagioclase. One candidate is whitlockite. Chao *et al.* [41] note that whitlockite is found in the 77215 mesostasis that often is associated with aggregates of plagioclase. Using a Nd concentration of 13 000 ppm and Lu content of 200 ppm [60] as an estimate of the whitlockite REE concentrations in 77215, and the Nd concentrations measured in 77215 plagioclase by Nakamura *et al.* [26], the concentration of Nd in our plagioclase separate could be explained by the presence of 0.13% whitlockite. Assuming an Nd/Lu ratio of 340 in the 77215 plagioclase, as seen in plagioclase from Mg-suite troctolite 76535 [61], then using the same mixing model, 0.13% whitlockite in our plagioclase separate would result in the Lu concentration increasing from 0.046 ppm for pure plagioclase to 0.3 ppm for the whitlockite contaminated separate. The measured concentration is 0.43 ppm, thus the contamination of the plagioclase separate with per-mil amounts of whitlockite is a possible explanation for the Sm and Nd concentration difference between the plagioclase measured here and that reported by Nakamura *et al.* [26].

In combination with the more extensive Rb-Sr dataset reported by Nakamura *et al.* [26], this study derives ages for 77215 of: Rb-Sr = 4374 ± 45 Ma, ^{147}Sm-^{143}Nd = 4283 ± 23 Ma, ^{146}Sm-^{142}Nd = 4348 Ma (103 Ma half-life) to 4413 Ma (68 Ma half-life) and Lu-Hf = 4421 ± 68 Ma. The ^{147}Sm-^{143}Nd age determined here is marginally younger, but within uncertainty of the 4373 ± 69 Ma age determined from refitting the data from Nakamura *et al.* [26], but our initial εNd is higher by approximately 2 ε units.

As with many studies of lunar highlands samples, this study finds discordant ages for different isotope systems when applied to exactly the same mineral and whole rock separates. Choosing which age best represents the crystallization age of the rock depends on applying subjective criteria. In reality, none of the ages need to reflect accurate crystallization ages as the lack of concordance from the different systems is a clear indication of disturbance of the radioisotope

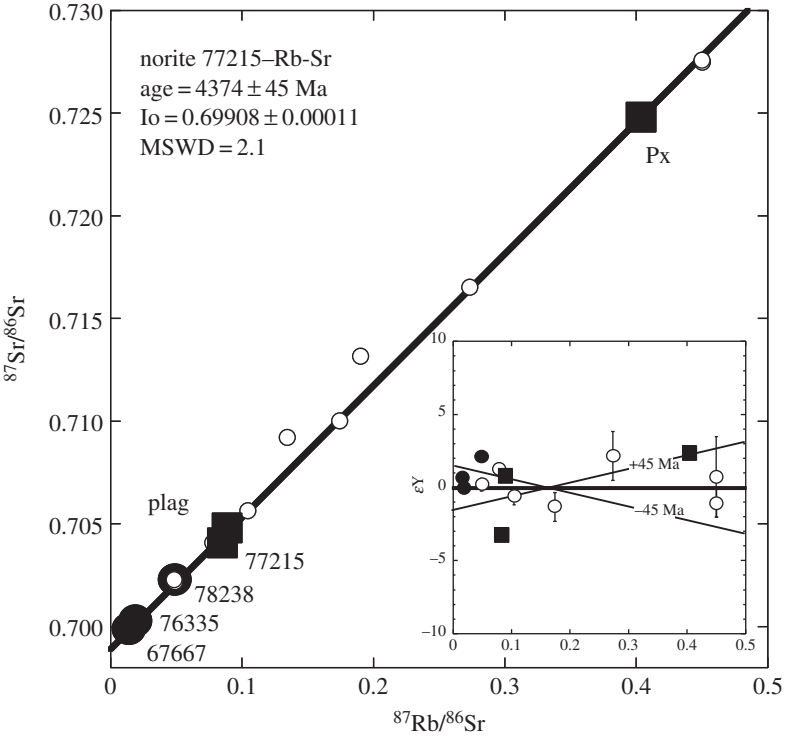

Figure 4. Rb-Sr isochron diagram for 77215 minerals and whole rock (squares) and Mg-suite whole rocks (filled circles). Additional data (open circles) from Nakamura *et al.* [26]. Inset shows deviation in parts in 10 000 of the individual data from the best fit line to the data reported here and all but the two high-density separates from Nakamura *et al.* [26]. Only data for 77215 are used to determine the lines shown in the figure.

systems. For 77215, post-crystallization disturbance of its isotope systematics is clearly indicated by *ca* 3.9–4.0 Ga ages from both Ar-Ar [42] and U-Pb [46]. Although they give overlapping ages, both the Rb-Sr and Lu-Hf data for 77215 scatter about any best fit line outside of the analytical error of the individual points reflective of disturbance whose effect on the age provided by these systems is uncertain. The most precise age for 77215 is the ^{147}Sm-^{143}Nd age of 4283 ± 23 Ma, but this age is the youngest of all the ages determined here. While the Sm-Nd system is commonly suggested to be the most robust to resisting shock-related metamorphic disturbance, all the isochrons reported here depend on data for plagioclase, a mineral with a known low closure temperature and the propensity to turn to glass (maskelyite) during shock events. In addition, the plagioclase measured here, based on its REE concentrations, clearly cannot be pure plagioclase, but likely contains whitlockite, another mineral with a low closure temperature that is thus easily reset by shock. Our conclusion, unfortunately, has to be that the isotope systematics are disturbed and that the best estimate for the crystallization age of 77215 lies between its 4283 ± 23 Ma ^{147}Sm-^{143}Nd age and its 4421 ± 68 Ma Lu-Hf age.

This age range for 77215 overlaps with two other recently redated Mg-suite rocks, 76535 (^{147}Sm-^{143}Nd = 4306 ± 11 Ma [61]) and 78236 (^{147}Sm-^{143}Nd = 4334 ± 37 Ma [27]), and with recently determined ages for FANs 60025 (4360 ± 3 Ma [14]) and 60016 (4300 ± 32 Ma [13]). Several Mg-suite samples have provided younger ages, but only three, 15445,17 [22], 78236 [28] and 74217 [62] have provided ages as old as the older FANs (figure 1). The age determined for 72417 is based on Rb-Sr analyses mostly of different chips from this dunitic clast. The age of 15445 [22] is based on a Sm-Nd isochron that has highly scattered Rb-Sr systematics that do not support the Sm-Nd age. A second clast (15445,247) from the same sample provides a much younger

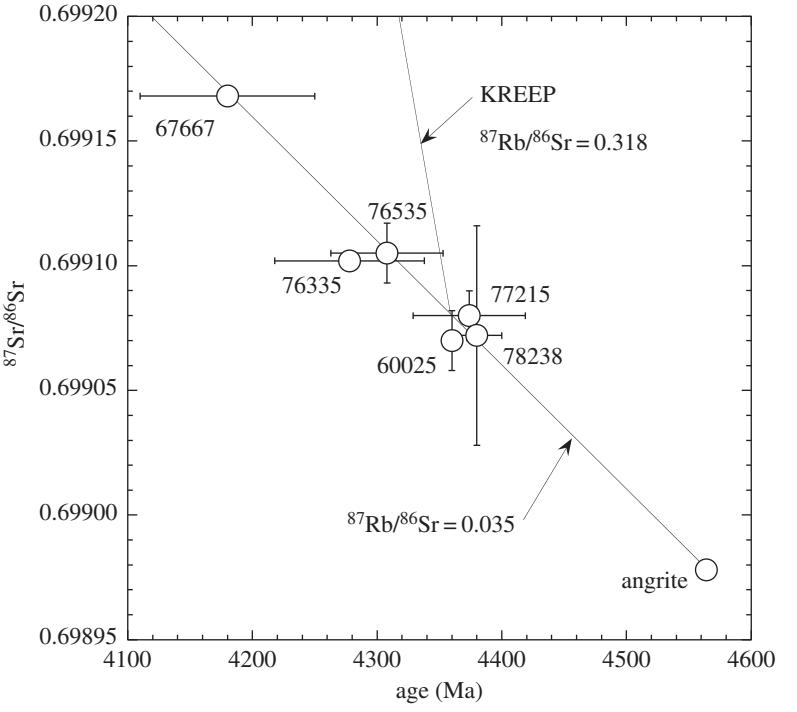

Figure 5. Sr isotope evolution diagram. Data for the angrite parent body initial from Hans *et al.* [63], 60025 from Carlson & Lugmair [17] and 76535 from Borg *et al.* [61]. The KREEP evolution line starts at the KREEP Sm-Nd model age of 4.36 Ga.

(4.28 ± 0.03 Ga) Sm-Nd age. The old age for 78236 has not been reproduced in other studies of this same sample [21] or its related sample 78238 [27]. Our conclusion is that the available chronological data for Mg-suite and FANs from the lunar highlands are not sufficiently precise, nor free of evidence for shock disturbance, to convincingly resolve either the age range of the FANs or whether Mg-suite rocks extend to ages older than the youngest FANs. What is clear is that none of the highlands samples studied so far provide convincing evidence for their formation prior to *ca* 4.4–4.5 Ga.

(b) History of the Mg-suite source

Regardless of the actual crystallization age of individual Mg-suite samples, their very elevated incompatible element abundances suggest the influence of a common, and highly differentiated, component in their magmatic source regions in the lunar interior. This is perhaps most clearly shown by the clustering of the initial $^{87}Sr/^{86}Sr$ of the individual Mg-suite samples, and FAN 60025, along a single Sr isotope evolution line evolving with $^{87}Rb/^{86}Sr = 0.035$ (figure 5). The estimated $^{87}Rb/^{86}Sr$ of KREEP is 0.318 [6], so the Mg-suite source could not have had such a high Rb/Sr ratio for more than 20–30 Ma prior to the crystallization age of the samples without evolving higher initial $^{87}Sr/^{86}Sr$ than measured for the samples (figure 5).

The derivation of the Mg-suite from a common source is supported by the excellent linearity of the whole rock Lu-Hf isochron defined by the data for the three Mg-suite samples with overlapping crystallization ages (excluding the younger 67667). The slope of this line corresponds to an age of 4347 ± 29 Ma with initial $\varepsilon Hf = -0.5 \pm 0.5$. This age has chronological significance only if the three rocks that define the line formed at the same time, from the same source, but we note the close correspondence of this age with the Sm-Nd and Lu-Hf model ages for KREEP [34,35,64].

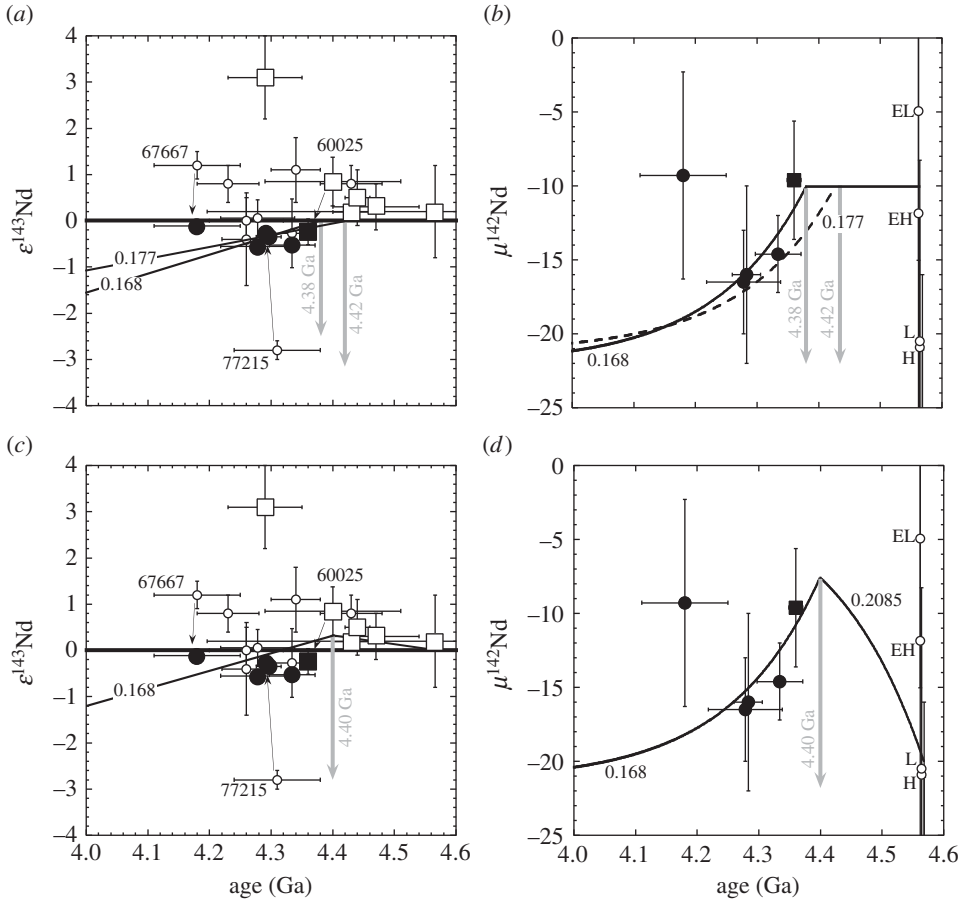

Figure 6. Initial ε^{143}Nd (parts in 10 000 deviation of initial $^{143}Nd/^{144}Nd$ from the average chondrite reference [45]) and μ^{142}Nd (ppm difference between the initial $^{142}Nd/^{144}Nd$ and the value the terrestrial standard would have at the formation age of the sample when age corrected on the assumption of a chondritic Sm/Nd ratio). Open circles are literature data as cited in the caption for figure 1. The open square is the data for FAN 60025 [17] and the filled square for the same sample from Borg *et al.* [25]. Filled circles are the Mg-suite data reported here. Evolution lines in parts (*a*,*b*) assume a source with chondritic Sm/Nd ($^{147}Sm/^{144}Nd = 0.196$; [45]) followed by evolution with the $^{147}Sm/^{144}Nd$ ratios shown by the labels on the lines/curves. Evolution lines in parts (*c*,*d*) assume an evolution starting from the average $^{142}Nd/^{144}Nd$ of ordinary chondrites (L, H) [31,47,50,65] with superchondritic Sm/Nd [47] until 4.4 Ga then with a $^{147}Sm/^{144}Nd = 0.168$, similar to estimated for KREEP [64]. Data for the average $^{142}Nd/^{144}Nd$ in enstatite chondrites (EL, EH) from Gannoun *et al.* [66].

Figure 6*a* shows that the more recent data for the initial $^{143}Nd/^{144}Nd$ of both FAN 60025 and the Mg-suite samples measured here converge towards values that are just slightly below those expected for a source evolving with chondritic Sm/Nd ratio. The new data thus do not support the observation of earlier studies that most highlands rocks had slightly superchondritic $^{143}Nd/^{144}Nd$ ratios at the time of their formation. We suggest that this difference likely reflects more accurate Nd isotope analyses obtained from the much larger sample sizes needed in the recent studies to obtain sufficiently precise $^{142}Nd/^{144}Nd$ data. The larger sample sizes allowed Nd to be measured as a metal instead of oxide ion, thereby minimizing correction for oxide interferences and Ce and Sm interference that is difficult to extract from Nd-oxide beams. The larger samples also are less sensitive to uncertainties resulting from processing blanks. The Mg-suite samples have Sm/Nd ratios that are too similar to define a precise whole rock isochron. The marginally negative initial εNd of the Mg-suite samples indicates their derivation from a

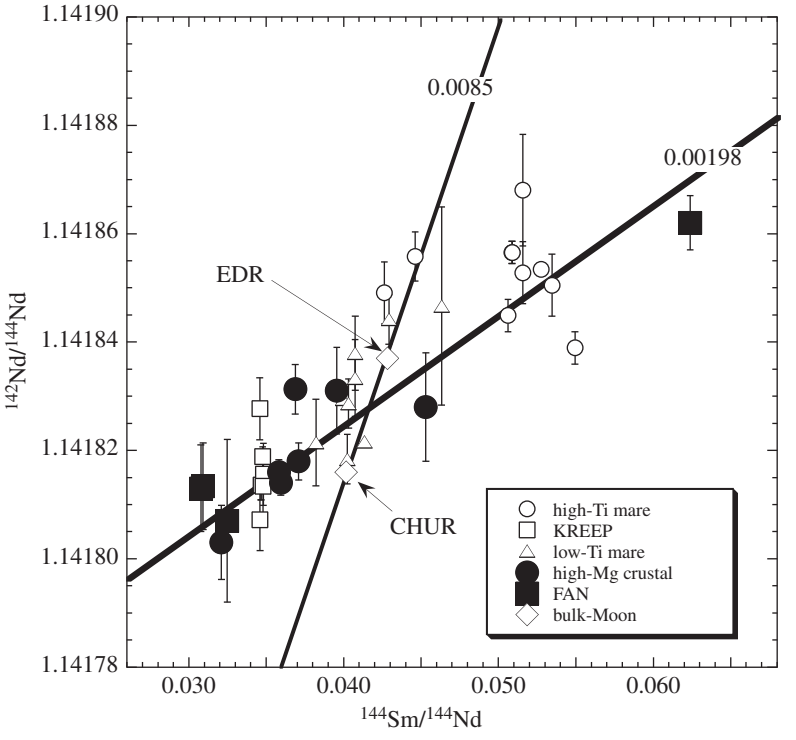

Figure 7. Measured Sm/Nd versus ^{142}Nd/^{144}Nd data for lunar igneous rocks. The best fit line through all the data has a slope of 0.00198 that corresponds to an age of 4352 Ma (103 Ma ^{146}Sm half-life) to 4416 Ma (68 Ma half-life). On this diagram, a slope of 0.0085 corresponds to the start of Solar System formation (4.567 Ga). Data from Rankenburg *et al.* [32], Boyet & Carlson [52], Brandon *et al.* [68], Borg *et al.* [14] and Borg *et al.* [61]. Two end member estimates are shown for the bulk-Moon composition, CHUR is the average of ordinary chondrites while EDR is the Early Depleted Reservoir, both defined in Boyet & Carlson [47]. The best fit line to the data passes 9 ppm below the EDR point in ^{142}Nd/^{144}Nd and hence about 9 ppm higher than the CHUR value.

light-REE-enriched source, consistent with their extreme enrichment in incompatible elements. Assuming that the Mg-suite samples obtained their incompatible elements from KREEP and taking typical estimates of the ^{147}Sm/^{144}Nd ratio for KREEP (0.168–0.177 [6,64]), the source model age for 77215 ranges from 4.38 to 4.42 Ga (figure 6*a*), ages that overlap the 4347 ± 29 Ma whole rock Lu-Hf isochron for the Mg-suite rocks. Figure 6*b*,*c* shows that the starting point of the lunar data in ^{142}Nd/^{144}Nd at *ca* 4.4 Ga appears to be of order 10 ppm lower than that of the accessible Earth, within the range measured for average enstatite chondrites [66]. This could reflect a nucleosynthetically induced offset in the initial ^{142}Nd/^{144}Nd of the Earth and Moon compared to the average value in ordinary chondrites [51,67], but the limited variation in initial ε^{143}Nd and μ^{142}Nd of the lunar crustal samples also allow the Moon to have an early evolution characterized by a superchondritic Sm/Nd ratio (figure 6*c*,*d* [52]).

(c) Simultaneous formation of ferroan anorthosite, Mg-suite, KREEP and mare basalt sources?

The many compositional distinctions between Mg-suite and FAN rocks show that their sources and/or petrogenetic processes clearly were distinct, but the initial Sr, Nd and Hf isotopic overlap at 4.35–4.40 Ga suggests that the distinct sources of the Mg-suite and FANs were not present in the lunar interior much before this time. This observation can be extended to other rock types on

Table 3. Age estimates for early lunar and terrestrial differentiation events.

observation	age (Ma)	references
Moon		
oldest concordant FAN ages	4360–4470	[14,18]
peak in lunar zircon age distribution	4320	[69]
oldest point on lunar zircon	4417	[70]
zircon Hf model ages	4380–4480	[71]
mare basalt ^{146}Sm-^{142}Nd source age	4320–4420	[31,32,52,68]
Pb model age for lunar highlands	4420	[72]
KREEP Sm-Nd and Lu-Hf model ages	4360–4440	[34,35,64]
^{182}Hf-^{182}W lunar model age	$<$4500 Ma	[73]
Earth		
Hf-W age of core formation	4450–4540	[74–76]
U-Pb age of the Earth	$\sim$ 4450	[77,78]
I-Pu-Xe age of the Earth's atmosphere	$\sim$ 4450	[79–81]
^{146}Sm-^{142}Nd model age for Isua	4350–4470	[82,83]
peak in oldest Hadean zircons	4350	[84]
^{146}Sm-^{142}Nd age for Nuvvuagittuq crust	4340–4400	[85]

the Moon by noting that the ^{146}Sm-^{142}Nd slope (0.00193 ± 0.00092) defined by the 77215 mineral data overlaps the 0.00153 ± 0.00035 slope defined by data for minerals from FAN 60025, and both of these overlap the slope of the Sm/Nd versus ^{142}Nd/^{144}Nd correlation defined by both KREEP and mare basalts (figure 7 [31,32,52,68]). The overlapping slopes of all the Sm/Nd versus ^{142}Nd/^{144}Nd data for this wide variety of lunar rock types suggest that their diverse sources formed over a relatively short time interval, as would be predicted by the magma ocean model for initial lunar differentiation. The slope of the best fit line through all the data shown in figure 7 is 0.00198 ± 0.00037, which corresponds to an age of 4416 (68 Ma half-life) to 4352 Ma (103 Ma half-life). The initial ^{142}Nd/^{144}Nd indicated by this 'planetary isochron' is 9 ppm lower than the accessible Earth would have at this time, within uncertainty of the 7 ppm deficit suggested by Sprung *et al.* [35]. The statistical uncertainty on the line corresponds to an error in the age on the order of 20–30 Ma. This 'planetary isochron', however, includes magmatic rocks whose measured Sm/Nd ratios almost certainly are different from those of their source rocks due to fractionation accompanying partial melting. Various attempts have been made to correct for the effect of this fractionation [31,32,35,52,68]. These approaches tend to lessen the slope of the Sm/Nd versus ^{142}Nd/^{144}Nd trend, making the inferred age younger by as much as 40 Ma. Given that this 'planetary isochron' consists of a wide variety of rock types formed over more than a billion years of lunar history, the true age uncertainty on this correlation is unclear. Nevertheless, the fact that all the data scatter along a similar trend is consistent with the idea that the source regions of all of these lunar rock types formed in a single event of limited duration. Although the absolute age is uncertain, the slope of this correlation clearly indicates that this event did not occur at Solar System formation, but was delayed by some 150–200 Ma.

A number of approaches to estimate the timing of the initial differentiation of the Moon return values closer to 4.4 Ga than above 4.5 Ga (table 3). This age could reflect a late formation for the Moon, a late start to magma ocean crystallization, or possibly that the Apollo lunar sample collection represents not the product of a global magma ocean, but instead a large impact melt 'lake' produced by a huge impact into the Moon, e.g. the proposed Procellarum basin [20,86].

An argument that this relatively young age may reflect the time of Moon formation is provided by the observation that a variety of approaches to estimate the age of early differentiation events on the Earth also provide ages approaching 4.4 Ga instead of more than 4.5 Ga (table 3). Concordance of early differentiation ages for the Earth and Moon is most simply explained if these ages are dating the time of the giant impact into the Earth that ejected the materials that now make up the Moon. Some of the terrestrial ages, for example, the Hf-W age of terrestrial core formation and the I-Pu-Xe age of the Earth's atmosphere are older than 4.5 Ga, but these conceivably could reflect memory of the Earth differentiation events that occurred prior to the giant impact and Moon formation [75,76,81,87]. Although all estimates of the time of Earth and Moon formation involve a good deal of interpretation, a number of approaches to estimate the time of earliest Earth and Moon differentiation point more towards ages less than 4.45 Ga than more than 4.5 Ga. The overlapping and relatively young age estimates for several early Earth/Moon differentiation events is compatible with Moon formation by a giant impact into the Earth some 150–200 Ma after the initiation of Solar System formation. This impact is the Moon forming event and likely the last major global differentiation event associated with the Earth accretion.

Acknowledgements. We thank Mary Horan and Tim Mock for their skilled oversight of the DTM chemistry and mass spectrometry laboratories. Detailed reviews from Thorsten Kleine and two anonymous reviewers are much appreciated.

Funding statement. This work was supported by NASA grant no. NNX08AH65G.

References

1. Wood JA, Dickey Jr JS, Marvin UB, Powell BN. 1970 Lunar Anorthosites and a geophysical model of the Moon. In *Proc. Apollo 11 Lunar Sci. Conf.*, pp. 965–988. New York, NY: Pergamon Press.
2. Walker D, Longhi J, Hays JF. 1975 Differentiation of a very thick magma body and implications for the source regions of mare basalts. In *Proc. 6th Lunar Sci. Conf.*, pp. 1103–1120. New York, NY: Pergamon Press.
3. Warren PH. 1985 The magma ocean concept and lunar evolution. *Annu. Rev. Earth Planet. Sci.* **13**, 201–240. (doi:10.1146/annurev.ea.13.050185.001221)
4. Dowty E, Prinz M, Keil K. 1974 Ferroan anorthosite: a widespread and distinctive lunar rock type. *Earth Planet. Sci. Lett.* **24**, 15–25. (doi:10.1016/0012-821X(74)90003-X)
5. Taylor SR, Jakes P. 1974 The geochemical evolution of the Moon. In *Proc. 5th Lunar Sci. Conf.*, pp. 1287–1305. New York, NY: Pergamon Press.
6. Warren PH, Wasson JT. 1979 The origin of KREEP. *Rev. Geophys. Space Phys.* **17**, 73–88. (doi:10.1029/RG017i001p00073)
7. James OB. 1980 Rocks of the early lunar crust. In *Proc. 11th Lunar Planet. Sci. Conf.*, pp. 365–393. New York, NY: Pergamon Press.
8. Shearer CK, Papike JJ. 2005 Early crustal building processes on the Moon: models for the petrogenesis of the magnesian suite. *Geochim. Cosmochim. Acta* **69**, 3445–3461. (doi:10.1016/j.gca.2005.02.025)
9. Hess PC. 1994 Petrogenesis of lunar troctolites. *J. Geophys. Res.* **99**, 19 083–19 093. (doi:10.1029/94JE01868)
10. Elkins-Tanton LT. 2008 Linked magma ocean solidification and atmospheric growth for Earth and Mars. *Earth Planet. Sci. Lett.* **271**, 181–191. (doi:10.1016/j.epsl.2008.03.062)
11. Solomon SC, Longhi J. 1977 Magma oceanography, 1. Thermal evolution. In *Proc. 8th Lunar Planet. Sci. Conf.*, pp. 583–599. New York, NY: Pergamon Press.
12. Borg LE, Norman M, Nyquist LE, Bogard DD, Snyder GA, Taylor LA, Lindstrom MM. 1999 Isotopic studies of ferroan anorthosite 62236: a young lunar crustal rock from a light rare-earth-element-depleted source. *Geochim. Cosmochim. Acta* **63**, 2679–2691. (doi:10.1016/S0016-7037(99)00130-1)
13. Marks N, Borg LE, Gaffney AM, Schearer CK, Burger P. 2014 Additional evidence for young ferroan anorthositic magmatism on the Moon from Sm-Nd isotopic measurements of 60016 clast 3A. *Lunar Planet. Sci.* **45**, 1129.

14. Borg LE, Connelly JN, Boyet M, Carlson RW. 2011 Chronological evidence that the Moon is either young or did not have a global magma ocean. *Nature* **477**, 70–73. (doi:10.1038/nature10328)
15. Norman MD, Borg LE, Nyquist LE, Bogard DD. 2003 Chronology, geochemistry, and petrology of a ferroan noritic anorthosite clast from Descartes breccia 67215: clues to the age, origin, structure, and impact history of the lunar crust. *Meteorit. Planet. Sci.* **38**, 645–661. (doi:10.1111/j.1945-5100.2003.tb00031.x)
16. Nyquist L *et al.* 2006 Feldspathic clasts in Yamato-86032: remnants of the lunar crust with implications for its formation and impact history. *Geochim. Cosmochim. Acta* **70**, 5990–6015. (doi:10.1016/j.gca.2006.07.042)
17. Carlson RW, Lugmair GW. 1988 The age of ferroan anorthosite 60025: oldest crust on a young Moon? *Earth Planet. Sci. Lett.* **90**, 119–130. (doi:10.1016/0012-821X(88)90095-7)
18. Nyquist LE, Shih C-Y, Reese YD, Park J, Bogard DD, Garrison DH, Yamaguchi A. 2010 Lunar crustal history recorded in lunar anorthosites. *Lunar Planet. Sci.* **41**, 1383.
19. Alibert C, Norman MD, McCulloch MT. 1994 An ancient Sm-Nd age for a ferroan noritic anorthosite clast from lunar breccia 67016. *Geochim. Cosmochim. Acta* **58**, 2921–2926. (doi:10.1016/0016-7037(94)90125-2)
20. Carlson RW, Lugmair GW. 1981 Sm-Nd age of lherzolite 67667: implications for the processes involved in lunar crustal formation. *Earth Planet. Sci. Lett.* **56**, 1–8. (doi:10.1016/0012-821X(81)90112-6)
21. Carlson RW, Lugmair GW. 1981 Time and duration of lunar highlands crust formation. *Earth Planet. Sci. Lett.* **52**, 227–238. (doi:10.1016/0012-821X(81)90177-1)
22. Shih CY, Nyquist LE, Dasch EJ, Bogard DD, Bansal BM, Wiesmann H. 1993 Ages of pristine noritic clasts from lunar breccias 15445 and 15455. *Geochim. Cosmochim. Acta* **57**, 915–931. (doi:10.1016/0016-7037(93)90178-Y)
23. Lugmair GW, Marti K, Kurtz JP, Scheinin NB. 1976 History and genesis of lunar troctolite 76535 or: how old is old? In *Proc. 7th Lunar Sci. Conf.*, pp. 2009–2033. New York, NY: Pergamon Press.
24. Edmunson J, Nyquist LE, Borg LE. 2007 Sm-Nd isotopic systematics of troctolite 76335. *Lunar Planet. Sci.* **42**, 2767.
25. Borg LE, Connelly J, Cassata W, Gaffney AM, Carlson RW, Papanastassiou D, Ramon E, Lindval R, Bizzarro M. 2013 Evidence for widespread magmatic activity at 4.36 Ga in the lunar highlands from young ages determined on troctolite 76535. *Lunar Planet. Sci.* **44**, 1563.
26. Nakamura N, Tatsumoto M, Nunes PD, Unruh DM, Schwab AP, Wildeman TR. 1976 4.4 b.y.-old clast in Boulder 7, Apollo 17: a comprehensive chronological study by U-Pb, Rb-Sr and Sm-Nd methods. In *Proc. 7th Lunar Sci. Conf.*, pp. 2309–2333. New York, NY: Pergamon Press.
27. Edmunson J, Borg LE, Nyquist LE, Asmerom Y. 2009 A combined Sm–Nd, Rb–Sr, and U–Pb isotopic study of Mg-suite norite 78238: further evidence for early differentiation of the Moon. *Geochim. Cosmochim. Acta* **73**, 514–527. (doi:10.1016/j.gca.2008.10.021)
28. Nyquist LE, Reimold WU, Bogard DD, Wooden JL, Bansal BM, Wiesmann H, Shih C-Y. 1981 A comparative Rb-Sr, Sm-Nd, and K-Ar study of shocked norite 78236: evidence for slow cooling in the lunar crust? In *Proc. 12th Lunar Planet. Sci. Conf.*, pp. 67–97. New York, NY: Pergamon Press.
29. Papanastassiou DA, Wasserburg GJ. 1976 Rb-Sr age of troctolite 76535. In *Proc. 7th Lunar Sci. Conf.*, pp. 2035–2054. New York, NY: Pergamon Press.
30. James OB, McGee JJ, Lindstrom MM. 1991 Lunar ferroan anorthosite 60025: petrology and chemistry of mafic lithologies. *Proc. Lunar Planet. Sci. Conf.* **21**, 63–87.
31. Nyquist LE, Wiesmann H, Bansal B, Shih C-Y, Keith JE, Harper CL. 1995 ^{146}Sm-^{142}Nd formation interval for the lunar mantle. *Geochim. Cosmochim. Acta* **59**, 2817–2837. (doi:10.1016/0016-7037(95)00175-Y)
32. Rankenburg K, Brandon AD, Neal CR. 2006 Neodymium isotope evidence for a chondritic composition of the Moon. *Science* **312**, 1369–1372. (doi:10.1126/science.1126114)
33. Sprung P, Scherer EE, Upadhyay D, Leya I, Mezger K. 2010 Non-nucleosynthetic heterogeneity in non-radiogenic stable Hf isotopes: Implications for early Solar System chronology. *Earth Planet. Sci. Lett.* **295**, 1–11. (doi:10.1016/j.epsl.2010.02.050)
34. Gaffney AM, Borg LE. 2013 A young age for KREEP formation determined from Lu-Hf isotope systematics of KREEP basalts and Mg-suite samples. *Lunar Planet. Sci.* **44**, 1714.

35. Sprung P, Kleine T, Scherer EE. 2013 Isotopic evidence for chondritic Lu/Hf and Sm/Nd of the Moon. *Earth Planet. Sci. Lett.* **380**, 77–87. (doi:10.1016/j.epsl.2013.08.018)
36. Warren PH, Wasson JT. 1977 Pristine nonmare rocks and the nature of the lunar crust. In *Proc. 8th Lunar Sci. Conf.*, pp. 2215–2235. New York, NY: Pergamon Press.
37. McCallum IS, Mathez EA. 1975 Petrology of noritic cumulates adn a partial melting model for the genesis of Fra Mauro basalts. In *Proc. 6th Lunar Sci. Conf.*, pp. 395–414. New York, NY: Pergamon Press.
38. Aeschlimann U, Eberhardt P, Geiss J, Grogler N, Kurtz J, Marti K. 1982 On the age of cumulate norite 78236. *Lunar Planet. Sci.* **13**, 1–2.
39. Premo WR, Tatsumoto M. 1991 U-Th-Pb isotopic systematics of lunar norite 78235. In *Proc. 21st Lunar Planet. Sci. Conf.*, pp. 89–100. Houston, TX: Lunar and Planetary Institute.
40. Hansen EC, Smith JV, Steele IM. 1980 Petrology and mineral chemistry of 67667, a unique feldspathic lherzolite. In *Proc. 11th Lunar Planet. Sci. Conf.*, pp. 523–533. New York, NY: Pergamon Press.
41. Chao ECT, Minkin JA, Thompson CL. 1976 The petrology of 77215, a noritic impact breccia. In *Proc. 7th Lunar Sci. Conf.*, pp. 2287–2308.
42. Stettler A, Eberhardt P, Geiss JJ, Grogler N. 1974 ^{39}Ar-^{40}Ar ages of samples from the Apollo 17 Station 7 boulder and implications for its formation. *Earth Planet. Sci. Lett.* **23**, 453–461. (doi:10.1016/0012-821X(74)90135-6)
43. Ludwig KR. 1991 ISOPLOT: a plotting and regression program for radiogenic-isotope data. *US Geol. Surv. Open-File Rep.* **91–445**, 39pp.
44. Minster J-F, Birck J-L, Allegre CJ. 1982 Absolute age of formation of chondrites studied by the ^{87}Rb-^{87}Sr method. *Nature* **300**, 414–419. (doi:10.1038/300414a0)
45. Bouvier A, Vervoort JD, Patchett PJ. 2008 The Lu-Hf and Sm-Nd isotopic composition of CHUR: constraints from unequilibrated chondrites and implications for the bulk composition of terrestrial planets. *Earth Planet. Sci. Lett.* **273**, 48–57. (doi:10.1016/j.epsl.2008.06.010)
46. Nunes PD, Tatsumoto M, Unruh DM. 1974 U-Th-Pb and Rb-Sr systematics of Apollo 17 boulder 7 from the North Massif of the Taurus-Littrow Valley. *Earth Planet. Sci. Lett.* **23**, 445–452. (doi:10.1016/0012-821X(74)90134-4)
47. Boyet M, Carlson RW. 2005 ^{142}Nd evidence for early (>4.53 Ga) global differentiation of the silicate Earth. *Science* **309**, 576–581. (doi:10.1126/science.1113634)
48. Carlson RW, Czamanske G, Fedorenko V, Ilupin I. 2006 A comparison of Siberian meimechites and kimberlites: implications for the source of high-Mg alkalic magmas and flood basalts. *Geochem. Geophys. Geosystems* **7**. (doi:10.1029/2006GC001342)
49. Connelly JN, Ulfbeck DG, Thrane K, Bizzarro M, Housh T. 2006 A method for purifying Lu and Hf for analyses by MC-ICP-MS using TODGA resin. *Chem. Geol.* **233**, 126–136. (doi:10.1016/j.chemgeo.2006.02.020)
50. Carlson RW, Boyet M, Horan M. 2007 Chondrite barium, neodymium, and samarium isotopic heterogeneity and early earth differentiation. *Science* **316**, 1175–1178. (doi:10.1126/science.1140189)
51. Qin L, Carlson RW, Alexander CMO'D. 2011 Correlated nucleosynthetic isotopic variability in Cr, Sr, Ba, Sm, Nd and Hf in Murchison and QUE 97008. *Geochim. Cosmochim. Acta* **75**, 7806–7828. (doi:10.1016/j.gca.2011.10.009)
52. Boyet M, Carlson RW. 2007 A highly depleted moon or a non-magma ocean origin for the lunar crust? *Earth Planet. Sci. Lett.* **262**, 505–516. (doi:10.1016/j.epsl.2007.08.009)
53. Lugmair GW, Marti K. 1978 Lunar initial ^{143}Nd/^{144}Nd: differential evolution of the lunar crust and mantle. *Earth Planet. Sci. Lett.* **39**, 349–357. (doi:10.1016/0012-821X(78)90021-3)
54. Scherer E, Muenker C, Mezger K. 2001 Calibration of the lutetium-hafnium clock. *Science* **293**, 683–687. (doi:10.1126/science.1061372)
55. Soderlund U, Patchett PJ, Vervoort JD, Isachen CE. 2004 The ^{176}Lu decay constant determined by Lu-Hf and U-Pb isotope systematics of Precambrian mafic intrusions. *Earth Planet. Sci. Lett.* **219**, 311–324. (doi:10.1016/S0012-821X(04)00012-3)
56. Friedman AM, Milsted J, Metta D, Henderson D, Lerner J, Harkness AL, Rokop DJ. 1966 Alpha decay half-lives of ^{148}Gd, ^{150}Gd and ^{146}Sm. *Radiochim. Acta* **5**, 192–194.
57. Boyet M, Carlson RW, Horan MF. 2010 Old Sm-Nd ages for cumulate eucrites and redetermination of the Solar System initial ^{146}Sm/^{144}Sm ratio. *Earth Planet. Sci. Lett.* **291**, 172–181. (doi:10.1016/j.epsl.2010.01.010)

58. Kinoshita N *et al.* 2012 A shorter ^{142}Nd half-life measured and implications for ^{146}Sm-^{142}Nd chronology in the Solar System. *Science* **335**, 1614–1617. (doi:10.1126/science.1215510)
59. Fletcher IR, Rosman KJR. 1982 Precise determination of initial εNd from Sm-Nd isochron data. *Geochim. Cosmochim. Acta* **46**, 1983–1987. (doi:10.1016/0016-7037(82)90138-7)
60. Jolliff BL, Haskin LA, Colson RO, Wadhwa M. 1993 Partitioning in REE-saturating minerals: Theory, experiment, and modelling of whitlockite, apatite, and evolution of lunar residual magmas. *Geochim. Cosmochim. Acta* **57**, 4069–4094. (doi:10.1016/0016-7037(93)90354-Y)
61. Borg LE, Connelly JN, Gaffney AM, Carlson RW, Cassata W, Papanastassiou DA, Wasserburg GJ, Bizzaro M. Submitted. Implications for the differentiation history of the Moon from the chronology of troctolite 76535. *Earth Planet. Sci. Lett.*
62. Papanastassiou DA, Wasserburg GJ. 1975 Rb-Sr study of a lunar dunite and evidence for early lunar differentiates. In *Proc. 6th Lunar Sci. Conf.*, pp. 1467–1490. New York, NY: Pergamon Press.
63. Hans U, Kleine T, Bourdon B. 2013 Rb-Sr chronology of volatile depletion in differentiated protoplanets: BABI, ADOR and ALL revisited. *Earth Planet. Sci. Lett.* **374**, 204–214. (doi:10.1016/j.epsl.2013.05.029)
64. Lugmair GW, Carlson RW. 1978 The Sm-Nd history of KREEP. *Proc. Lunar Planet. Sci. Conf.* **9**, 689–704.
65. Andreasen R, Sharma M. 2006 Solar nebula heterogeneity in p-process samarium and neodymium isotopes. *Science* **314**, 806–809. (doi:10.1126/science.1131708)
66. Gannoun A, Boyet M, Rizo H, Goresy AE. 2011 ^{146}Sm-^{142}Nd systematics measured in enstatite chondrites reveals a heterogeneous distribution of ^{142}Nd in the solar nebula. *Proc. Natl Acad. Sci. USA* **108**, 7693–7697. (doi:10.1073/pnas.1017332108)
67. Boyet M, Gannoun A. 2013 Nucleosynthetic Nd isotope anomalies in primitive enstatite chondrites. *Geochim. Cosmochim. Acta* **121**, 652–666. (doi:10.1016/j.gca.2013.07.036)
68. Brandon AD, Lapen TJ, Debaille V, Beard BL, Rankenburg K, Neal C. 2009 Re-evaluating ^{142}Nd/^{144}Nd in lunar mare basalts with implications for the early evolution and bulk Sm/Nd of the Moon. *Geochim. Cosmochim. Acta* **73**, 6421–6445. (doi:10.1016/j.gca.2009.07.015)
69. Grange ML, Nemchin AA, Pidgeon RT, Merle RE, Timms NE. 2013 What lunar zircon ages can tell? *Lunar Planet. Sci.* **44**, 1884.
70. Nemchin A, Timms N, Pidgeon R, Geisler T, Reddy S, Meyer C. 2009 Timing of crystallization of the lunar magma ocean constrained by the oldest zircon. *Nat. Geosci.* **2**, 133–136. (doi:10.1038/ngeo417)
71. Taylor DJ, McKeegan KD, Harrison TM. 2009 Lu-Hf zircon evidence for rapid lunar differentiation. *Earth Planet. Sci. Lett.* **279**, 157–164. (doi:10.1016/j.epsl.2008.12.030)
72. Tera F, Wasserburg GJ. 1974 U-Th-Pb systematics on lunar rocks and inferences about lunar evolution and the age of the moon. In *Proc. 5th Lunar Sci. Conf.*, pp. 1571–1599. New York, NY: Pergamon Press.
73. Touboul M, Kleine T, Bourdon B, Palme H, Wieler R. 2007 Late formation and prolonged differentiation of the Moon inferred from W isotopes in lunar metals. *Nature* **450**, 1206–1209. (doi:10.1038/nature06428)
74. Halliday AN, Kleine T. 2005 *Meteorites and the timing, mechanisms, and conditions of terrestrial planet accretion and early differentiation*. In *Meteorites and the Early Solar System II* (eds DS Lauretta, HY McSween Jr). Tucson, AZ: The University of Arizona Press.
75. Kleine T, Touboul M, Bourdon B, Nimmo F, Mezger K, Palme H, Jacobsen SB, Yin QZ, Halliday AN. 2009 Hf-W chronology of the accretion and early evolution of asteroids and terrestrial planets. *Geochim. Cosmochim. Acta* **73**, 5150–5188. (doi:10.1016/j.gca.2008.11.047)
76. Rudge JF, Kleine T, Bourdon B. 2010 Broad bounds on Earth's accretion and core formation constrained by geochemical models. *Nat. Geosci.* **3**, 439–443. (doi:10.1038/ngeo872)
77. Patterson C. 1956 Age of meteorites and the Earth. *Geochim. Cosmochim. Acta* **10**, 230. (doi:10.1016/0016-7037(56)90036-9)
78. Allègre CJ, Mahnes G, Gopel C. 2008 The major differentiation of the Earth at ~4.45 Ga. *Earth Planet. Sci. Lett.* **267**, 353–364. (doi:10.1016/j.epsl.2007.11.056)
79. Staudacher T, Allegre CJ. 1982 Terrestrial xenology. *Earth Planet. Sci. Lett.* **60**, 389–406. (doi:10.1016/0012-821X(82)90075-9)

80. Pepin RO, Porcelli D. 2006 Xenon isotope systematics, giant impacts, and mantle degassing on the early Earth. *Earth Planet. Sci. Lett.* **250**, 470–485. (doi:10.1016/j.epsl.2006.08.014)
81. Mukhopadhyay S. 2012 Early differentiation and volatile accretion in deep mantle neon and xenon. *Nature* **486**, 101–104. (doi:10.1038/nature11141)
82. Caro G, Bourdon B, Birck J-L, Moorbath S. 2006 High-precision $^{142}Nd/^{144}Nd$ measurements in terrestrial rocks: constraints on the early differentiation of the Earth's mantle. *Geochim. Cosmochim. Acta* **70**, 164–191. (doi:10.1016/j.gca.2005.08.015)
83. Rizo H, Boyet M, Blichert-Toft J, Rosing M. 2011 Combined Nd and Hf isotope evidence for deep-seated source of Isua lavas. *Earth Planet. Sci. Lett.* **312**, 267–279. (doi:10.1016/j.epsl.2011.10.014)
84. Holden P, Lanc P, Ireland TR, Harrison TM, Foster JJ, Bruce Z. 2009 Mass-spectrometric mining of Hadean zircons by automated SHRIMP multi-collector and single-collector U/Pb zircon age dating: the first 100,000 grains. *Int. J. Mass Spec.* **286**, 53–63. (doi:10.1016/j.ijms.2009.06.007)
85. O'Neil J, Carlson RW, Paquette J-L, Francis D. 2012 Formation age and metamorphic history of the Nuvvuagittuq greenstone belt. *Precambrian Res.* **220–221**, 23–44. (doi:10.1016/j.precamres.2012.07.009)
86. Cadogan PH. 1974 Oldest and largest lunar basin? *Nature* **250**, 315–316. (doi:10.1038/250315a0)
87. Halliday AN. 2004 Mixing, volatile loss and compositional change during impact-driven accretion of the Earth. *Nature* **427**, 505–509. (doi:10.1038/nature02275)